

Pions near the chiral critical point

M Hippert¹, E S Fraga¹ and E M Santos²

¹ Instituto de Física, Universidade Federal do Rio de Janeiro, Caixa Postal 68528, 21941-972, Rio de Janeiro, RJ, Brazil

² Instituto de Física, Universidade de São Paulo, Caixa Postal 66318, 05314-970, São Paulo, SP, Brazil.

E-mail: hippert@if.ufrj.br

Abstract. It is an exciting possibility that the QCD critical point can be found in ultrarelativistic heavy-ion collision experiments (HICs). While quantities such as some event-by-event moments of specific observables should display strong non-monotonic behavior near the critical point and could, hence, be used as signatures of criticality, it is not clear that this behavior could effectively be observed in the highly non-ideal scenario of HICs. We here employ Monte Carlo simulations to test second-order moments of pion observables as possible signatures of the critical point while taking into account some realistic ingredients, similar to the ones found in HICs. We make use of simplified models to introduce spurious contributions and dynamical effects.

1. Introduction

The QCD chiral phase diagram might present a second-order critical endpoint (CEP) accessible to current heavy-ion collision experiments (HICs) [1, 2, 3, 4, 5]. The experimental discovery of such a feature of the QCD phase diagram would be of huge importance and a large amount of literature has been dedicated to the study of the effects of the CEP in experimentally accessible observables. Among possible signatures for searching the CEP, it has been proposed that critical fluctuations in its neighborhood could have a large impact upon moments of the event-by-event distribution of observables [6, 7, 8, 9, 10, 11, 12, 13, 14, 15]. This would result in a non-monotonic increase of these moments as experimental conditions probe this region of the QCD phase diagram.

However, it is not at all obvious that the non-monotonic increase in these quantities could be visible in the environment of the small amount of plasma produced in HICs [16, 17, 18], especially if effects from dynamics and spurious contributions are considered. In the following, we study the behavior of second-order moments of pions near criticality within a simplified model [19]. In order to introduce some of the expected experimental limitations of a real experiments, we apply Monte Carlo techniques.

2. Effective theory

Our choice of approach for studying the critical behavior of the observables of interest is taken from Refs. [6, 8]. In this context, the chiral field σ is used as an order parameter for the chiral phase transition. In the second-order CEP, its mass, m_σ , is expected to vanish, thus giving rise to strong long-wavelength fluctuations and the divergence of the corresponding correlation



length $\xi \approx 1/m_\sigma$. In order to describe this behavior, a classical treatment is applied along with a homogeneous approximation $\sigma(x) \approx \sigma_0$. The probability distribution for σ_0 is given by

$$P[\sigma_0] = e^{-\Omega[\sigma_0]/T}, \quad (1)$$

where T is the temperature and the effective potential Ω is expanded in powers of σ_0 ,

$$\Omega[\sigma_0] \approx V \frac{1}{2} m_\sigma^2 \sigma_0^2 + \mathcal{O}(\sigma_0^3). \quad (2)$$

Interaction with pions is only introduced as a shift in the pion mass squared, m_π^2 ,

$$\mathcal{L}_{int} = -G \sigma_0 \vec{\pi} \cdot \vec{\pi} + \mathcal{O}(\phi^4), \quad (3)$$

or equivalently,

$$m_\pi^2 = m_\pi^{(0)2} + 2G \sigma_0, \quad (4)$$

where a value of $G \approx 300$ MeV near the CEP is taken from [6].

Eqs. (1), (2) and (4) yield a probability distribution for m_π^2 . This distribution turns out to be Gaussian within the present approximations, with a width $2G\xi\sqrt{T/V}$, where V is the system volume. This picture enables us to have a grasp on critical correlations among pions while essentially regarding them as free particles. As the pion mass fluctuates, it collectively affects the pion multiplicity and transverse momentum distribution, generating event-by-event correlations among observables. In particular, it can be shown that

$$\langle \Delta n_p \Delta n_k \rangle \approx \frac{(G\xi)^2}{TV} \frac{1}{\omega_p} \frac{1}{\omega_k} f_p(1+f_p) f_k(1+f_k) + \mathcal{O}((\delta m_\pi^2)^4), \quad (5)$$

where k and p denote distinct (free) one-particle pionic states, of energy ω_p and ω_k and occupation numbers n_p and n_k , respectively, and $f_p = (e^{\omega_p/T} - 1)^{-1}$. The correlation in Eq. (5) can be used to calculate critical contributions to second-order moments of observables of pions. Its quadratic dependence in ξ indicates an enhancement of these contributions as the CEP is approached and ξ increases.

The picture outlined above enables the construction of a very simple Monte Carlo algorithm for generating distributions of pions displaying the desired critical correlations [19]:

- (i) draw m_π^2 from a Gaussian distribution of width $2G\xi\sqrt{T/V}$;
- (ii) for each mode p , draw an occupation number n_p according to the Boltzmann factor $e^{-\omega_p n_p/T}$.

In order to have a finite number of modes, it is necessary to impose boundary conditions. We impose Dirichlet boundary conditions on a sphere, partially introducing finite-size effects into our treatment.

3. Heavy-ion collisions

Since ξ increases near the CEP, Eq. (5) shows that second-order moments of pions should exhibit non-monotonic behavior as the freeze-out conditions of the plasma formed in HICs approach and depart from its neighborhood. Our goal is to test whether this behavior is sufficiently strong to be experimentally detected in realistic conditions, providing signatures of the critical point.

Our simulations aim at reproducing freeze-out conditions from the RHIC Beam Energy Scan program. We choose parameters inspired on results from STAR regarding $Au + Au$ collisions at center-of-mass energy $\sqrt{s_{NN}} = 7.7$ GeV in the 0–5% centrality class and pretend the CEP

is near the corresponding freeze-out parameters. For this centrality and this center-of-mass energy, the freeze-out temperature and plasma radius are in the ranges $T_{f.o.} \approx 110 - 150$ MeV and $R_{f.o.} \approx 6 - 8$ fm, taking different values for chemical and kinetic freeze-out [20, 21]. We take $T = 130$ MeV and $R = 6.8$ fm and restrict our analysis to pions of transverse momentum $p_T \leq 1$ GeV and pseudo-rapidity in the window $|y| \leq 0.5$. As to introduce some realism, we include limitations in the growth of ξ due to critical dynamics and fluctuations of the freeze-out parameters [19].

3.1. Fluctuations of freeze-out parameters

The experimental study of event-by-event correlations implies a sample of events. However, in HICs, it is not at all possible to prepare or post-select identical events. While centrality binning (and possibly other kinds of post-selection) can be used to reduce this effect, experimental events in a given sample will always vary in initial conditions and evolution, so that freeze-out parameters will inevitably fluctuate among them. Since these fluctuations affect the resulting distribution of particles as a whole, they can generate collective fluctuations that provide a background to critical fluctuations in this kind of analysis.

The final volume and geometry of the plasma, for instance, depend on initial conditions and should fluctuate accordingly. As a simplified model, we consider the colliding nuclei as disks, due to Lorentz contraction, and suppose the plasma to be a sphere of volume proportional to the intersection area between the nuclei at the instant of collision. A probability distribution for the freeze-out radius $R_{f.o.}$ is then obtained by considering a linear probability distribution for the impact parameter $\mathcal{P}(b) \propto b$. The intersection area can be easily found as a function of the impact parameter b and the nuclear radius R_N ,

$$A(b, R_N) = 2R_N^2 \cos^{-1} \left(\frac{b}{2R_N} \right) - b \sqrt{R_N^2 - \frac{b^2}{4}}, \quad (6)$$

while the proportionality constant can be found by fixing the plasma radius for a given centrality class (we choose $R_{f.o.} = 6.8$ fm for 0 – 5% centrality) [19]. Our estimate of R_N is the measured parameter $r_0 = 6.38$ fm of the Woods-Saxon nuclear density profile for the gold nucleus [22, 23].

While lacking a simplified model for temperature fluctuations and its relation to volume fluctuations, we just assume the freeze-out temperature to fluctuate according to a Gaussian distribution of 5% width, which we believe to be a moderate choice. Since pions are not directly sensitive to the baryonic chemical potential μ_B , fluctuations of its freeze-out value are not taken into account.

3.2. Critical slowing down

As explicit in Eq. (5), second order correlations exhibit an approximately quadratic dependence on ξ . While in equilibrium and in the thermodynamic limit $\xi \rightarrow \infty$ as the CEP is approached, this cannot be the case for a real system with finite size and lifetime. Since ξ should not grow arbitrarily fast, as its equilibrium value increases towards infinity, so do the equilibration times, in what is known as critical slowing down [24]. This effect can significantly affect the proposed signatures of criticality [25].

In order to take this limitation into account, we use the treatment of Ref. [25] to find the time-dependence of ξ near the CEP, including several simplifying approximations and assumptions. With the purpose of using the Ising universality class of QCD, the system is considered to be in equilibrium until a sufficiently large value ξ_0 of the correlation length is reached, so that universality arguments apply. The system is also taken to cool down at a constant rate dT/dt , at constant baryonic chemical potential and exactly over the critical point, while the reduced temperature is taken to be proportional to the Ising reduced magnetic field when mapping the problem to the Ising Model [19].

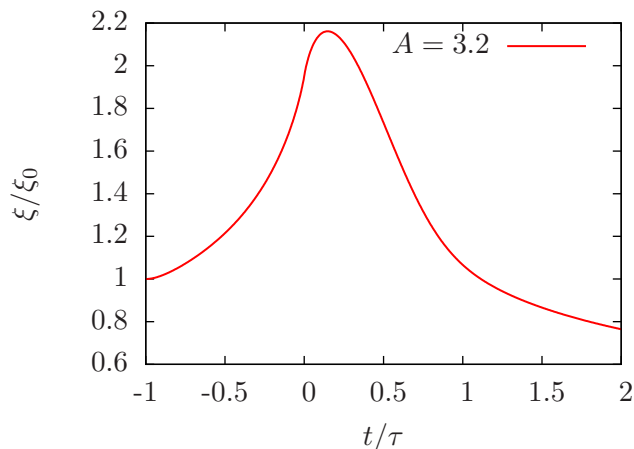


Figure 1. Evolution of the correlation length ξ in the most favorable scenario, with $A = A_{max} = 3.2$. Its value never exceeds $2.2 \xi_0$, being most likely under $1.8 \xi_0$, depending on at which instant t freeze-out occurs.

Besides universal parameters and the dimensionless constant A , there are two necessary scales that determine ξ as a function of time t : the cooling time $\tau := \frac{T_0 - T_E}{|dT/dt|}$, where T_E is the critical temperature and T_0 is the temperature above which the treatment can be applied, and the initial correlation length ξ_0 [19]. Since $\xi_0 > 1/T_E$, we take $\xi_0 = 1/120 \text{ MeV} = 1.6 \text{ fm}$ and, based on two-pion interferometry results for the lifetime of the system, we estimate the time scale between reaching ξ_0 and crossing the critical point as $\tau = 5.5 \text{ fm}$ [21]. The longer the correlation length has to respond to criticality and the smaller its initial value, the higher the factor $\xi(t)/\xi_0$ can get. We therefore consider these values to be very optimistic. While the dimensionless constant A is not estimated in Ref [25], it can be constrained by asking that the correlation length never increases above the speed of light. The greater its value, the faster ξ can grow. It can thus be shown that $A \leq A_{max} = 3.2$ [19].

Fig. 1 shows $\xi(t)$ for $A = A_{max}$ within this approach, with the system crossing the CEP at $t = 0$. It is clear that ξ should not grow by a factor larger than 2.2, reaching up to $\sim 3.5 \text{ fm}$. Since this value is smaller than the typical system radius, we believe dynamical effects to be more restraining than the finite size of the system.

4. Results

Finally, we make simulations of 10^6 events for various values of ξ , ranging from $\xi_0 = 1.6 \text{ fm}$ to $2.2 \times 1.6 \text{ fm} = 3.5 \text{ fm}$, and calculate, for each of them, the second-order moments $\langle(\Delta N)^2\rangle$ and $\langle(\Delta \bar{p}_T)^2\rangle$ for charged pions, where N is the particle multiplicity and \bar{p}_T is the mean transverse momentum among particles of a given event [19]. These moments are normalized by the appropriate power of $\langle N \rangle$ to cancel out system-size dependence.

Our results are shown in Fig. 2, as a function of the combination $\xi_\chi^2 := (G\xi)^2$. We choose to display them as relative variations with respect to the values for $\xi = 1.6 \text{ fm}$, revealing that the tested signatures can increase up to $\sim 10\%$ in the case of $\langle(\Delta N)^2\rangle$. A larger signal could be found for the mixed moment $\langle \Delta N \Delta \bar{p}_T \rangle$. However, since chemical and kinetic freeze-out occur separately, there should be no correlation between N and \bar{p}_T , so we believe this result to be artificial.

It is also interesting to find how these signatures depend on the instant of freeze-out. For that purpose, a linear fit can be made in Fig. 2 to extract the dependence of $\langle(\Delta N)^2\rangle/\langle(\Delta N)^2\rangle_0$ in ξ_χ^2 , which can be used along with the time dependence $\xi(t)$ obtained in Section 3.2. The result is shown in Fig. 3, with the time variable replaced by the difference between the critical and the freeze-out temperatures using $T_0 - T_E = 44 \text{ MeV}$. It should not be interpreted as the non-monotonic behavior expected as the beam energy of an experiment is varied, but rather as

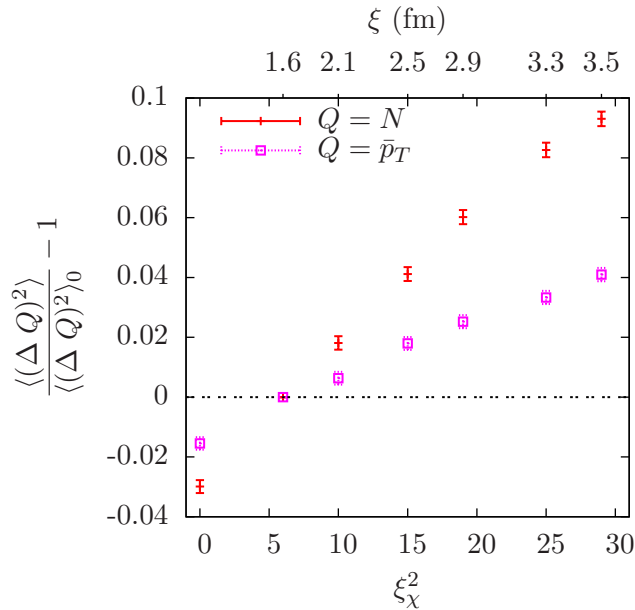


Figure 2. Signal as a function of ξ_χ^2 and ξ , in proportion to the reference value, taken at $\xi = 1.6$ fm. The variances of the charged pion multiplicity, N , and the average transverse momentum of charged pions for a single event, \bar{p}_T , are shown.

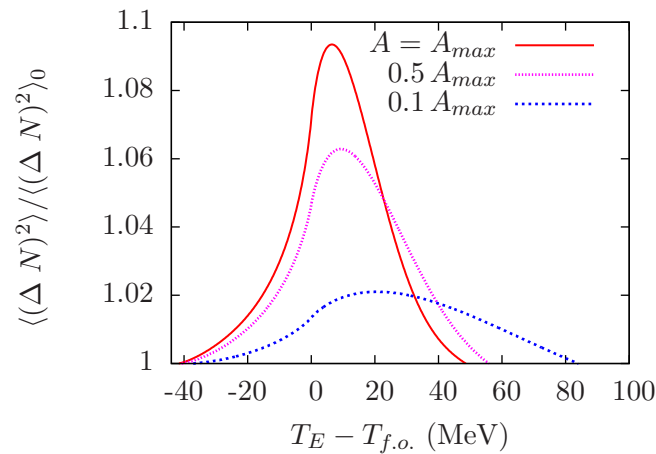


Figure 3. Behavior of the signal to baseline ratio of the variance of N as the freeze-out temperature is varied over a cooling trajectory which crosses the CEP at $T = T_E$, for different choices of the parameter A .

displaying the influence of the amount by which the system cools before freeze-out given that cooling occurs over the critical point. Different values of the parameter A are used and one should bear in mind that changing it has the same effect of changing the cooling time τ by the same factor.

5. Final remarks

In this work, we have analyzed second-order event-by-event moments of pions as signatures of the chiral critical point in HICs. It should be regarded as a first step towards a more realistic understanding of the impact of experimental limitations upon signals of the CEP in HICs. As such, it can and should be enhanced in many ways such as by including contributions from resonance decays, re-scattering and hydrodynamic flow. Since we have assumed perfect equilibrium (apart from Section 3.2), used very simple models and chosen optimistic values whenever estimates were necessary, our results should be regarded as limiting how optimistic one could be about the performance of tested signatures [19]. Results for higher-order moments and moments of protons, which should both yield stronger signatures [8, 9], are left for future developments.

Acknowledgments

This work was partially supported by CAPES, CNPq and FAPERJ.

References

- [1] Stephanov M 2006 *PoS LAT2006* 024 (*Preprint hep-lat/0701002*)
- [2] Rajagopal K 1995 (*Preprint hep-ph/9504310*)
- [3] Stephanov M A 2004 *Prog.Theor.Phys.Suppl.* **153** 139–156 (*Preprint hep-ph/0402115*)
- [4] Hatta Y and Ikeda T 2003 *Phys. Rev. D* **67**(1) 014028 URL <http://link.aps.org/doi/10.1103/PhysRevD.67.014028>
- [5] Fraga E S, Palhares L F and Sorensen P 2011 *Phys.Rev. C* **84** 011903 (*Preprint 1104.3755*)
- [6] Stephanov M A, Rajagopal K and Shuryak E V 1999 *Phys.Rev. D* **60** 114028 (*Preprint hep-ph/9903292*)
- [7] Stephanov M A 2002 *Phys.Rev. D* **65** 096008 (*Preprint hep-ph/0110077*)
- [8] Stephanov M 2009 *Phys.Rev.Lett.* **102** 032301 (*Preprint 0809.3450*)
- [9] Athanasiou C, Rajagopal K and Stephanov M 2010 *Phys.Rev. D* **82** 074008 (*Preprint 1006.4636*)
- [10] Mukherjee S, Venugopalan R and Yin Y 2015 (*Preprint 1506.00645*)
- [11] Antoniou N G, Diakonov F K and Saridakis E N 2007 *Nucl. Phys. A* **784** 536–550 (*Preprint hep-ph/0610382*)
- [12] Antoniou N G, Diakonov F K and Saridakis E N 2008 *Phys. Rev. C* **78** 024908 (*Preprint 0709.0339*)
- [13] Luo X (STAR) 2013 *Nucl. Phys. A* **904-905** 911c–914c [Central Eur. J. Phys.10,1372(2012)] (*Preprint 1210.5573*)
- [14] Adamczyk L *et al.* (STAR Collaboration) 2013 (*Preprint 1309.5681*)
- [15] Luo X (STAR) 2013 *PoS CPOD2013* 019 (*Preprint 1306.3106*)
- [16] Palhares L, Fraga E and Kodama T 2010 *J.Phys. G* **37** 094031
- [17] Kiriya O, Kodama T and Koide T 2006 (*Preprint hep-ph/0602086*)
- [18] Braun J, Klein B, Pirner H J and Rezaeian A 2006 *Phys.Rev. D* **73** 074010 (*Preprint hep-ph/0512274*)
- [19] Hippert M, Fraga E S and Santos E M 2015 (*Preprint 1507.04764*)
- [20] Chatterjee S, Das S, Kumar L, Mishra D, Mohanty B, Sahoo R and Sharma N 2014 *Adv.High Energy Phys.* **2014** 349013 URL <http://www.hindawi.com/journals/ahp/aa/349013/ref/>
- [21] Adamczyk L *et al.* (STAR Collaboration) 2014 (*Preprint 1403.4972*)
- [22] Vries H D, Jager C D and Vries C D 1987 *Atomic Data and Nuclear Data Tables* **36** 495 – 536 ISSN 0092-640X URL <http://www.sciencedirect.com/science/article/pii/0092640X87900131>
- [23] Jager C D, Vries H D and Vries C D 1974 *Atomic Data and Nuclear Data Tables* **14** 479 – 508 ISSN 0092-640X nuclear Charge and Moment Distributions URL <http://www.sciencedirect.com/science/article/pii/S0092640X74800021>
- [24] Hohenberg P and Halperin B 1977 *Rev.Mod.Phys.* **49** 435–479
- [25] Berdnikov B and Rajagopal K 2000 *Phys.Rev. D* **61** 105017 (*Preprint hep-ph/9912274*)